

Dominic O'Connor, John Kaiser Calautit, Ben Richard Hughes, A study of passive ventilation integrated with heat recovery, **Energy and Buildings**, Volume 82, October 2014, Pages 799-811, ISSN 0378-7788.



## A Study of Passive Ventilation Integrated with Heat Recovery

Dominic O'Connor<sup>a,\*</sup>, John Kaiser Calautit<sup>a</sup>, Ben Richard Hughes<sup>a</sup>

<sup>a</sup> School of Civil Engineering, University of Leeds, Leeds LS2 9JT, United Kingdom

\* Corresponding author: Tel: +44 7857883363, Email: [cn09dbo@leeds.ac.uk](mailto:cn09dbo@leeds.ac.uk)

### Abstract

To meet the demand for energy demand reduction in heating, ventilation and air-conditioning systems, a novel design incorporating a heat recovery device into a wind tower was proposed. The integrated system uses a rotary thermal wheel for heat recovery at the base of the wind tower. A 1:10 scale prototype of the system was created and tested experimentally in a closed-loop subsonic wind tunnel to validate the Computational Fluid Dynamics (CFD) investigation. Wind towers have been shown to be capable of providing adequate ventilation in line with British Standards and the Chartered Institution of Building Services Engineers (CIBSE) guidelines. Despite the blockage of the rotary thermal wheel, ventilation rates were above recommendations. In a classroom with an occupancy density of 1.8m<sup>2</sup>/person, the wind tower with rotary thermal wheel was experimentally shown to provide 9L/s per person at an inlet air velocity of 3m/s, 1L/s per person higher than recommended ventilation rates. This is possible with a pressure drop across the heat exchanger of 4.33Pa. In addition to sufficient ventilation, the heat in the exhaust airstreams was captured and transferred to the incoming airstream, raising the temperature 2°C, this passive recovery has the potential to reduce demand on space heating systems.

**Keywords:** air supply rate, CFD; natural ventilation; rotary wheel; wind tower; wind tunnel

# 1. Introduction

The statutory requirement to reduce UK greenhouse gas emissions by 80% from pre-1990 levels by 2050 is a major driving force in decreasing energy demand for the operation and maintenance of buildings in the UK (1). Space heating currently accounts for 40% of total energy demand in residential and service sector properties in the UK and other developed nations (2). A reduction in the energy required to heat domestic and non-domestic buildings, most commonly recognised as office, school and retail buildings, presents one part of a solution to reach the goal of cutting greenhouse gas emissions.

Mechanical ventilation fulfils many uses through the use of fans and blowers; circulating internal air back through the building or drawing external air into the building, removing stale and polluted air as well as conditioning the occupied space for thermal comfort. These processes are highly energy intensive. Mechanical ventilation systems which provide heating and cooling are commonly referred to as Heating, Ventilation, and Air-conditioning (HVAC) create a significant demand of the total energy used in many buildings (3). Natural ventilation uses pressure differences in and around a building to force external air into a building and draw internal air out, in this way no mechanical processes or energy input are required (4). Pressure differences created by wind flow around a building provide a higher level of ventilation compared to the pressure differences created by the buoyancy effect of warmed air (5).

Wind towers are a traditional Middle Eastern technology that utilises natural ventilation to encourage ventilation and cooling in buildings (6, 7). This technology has been used for many hundreds of years and has been adopted commercially in the UK (8). Wind towers have been proven as an effective replacement to air-handling units in schools and commercial office buildings in ventilating rooms during summer months (9). Wind towers are designed as a ventilation aid to bring in fresh air from outside and remove pollutants; therefore their use is generally limited to the cooling seasons in the UK, as can be seen in Figure 1. This is due to the potential for low incoming air

temperatures to cause thermal discomfort to the occupants and the perception that the use of natural ventilation solutions will increase heat loss and lead to increased energy costs which are unfavourable for many users. There are examples of wind towers in use in winter months but this is generally restricted (10). However, by restricting the use of natural ventilation methods during winter months, the concentration of pollutants have been seen to rise above the accepted guideline levels as stated by CIBSE and the Department for Education and Skills (DfES), which can lead to poor mental performance and ill health (11).

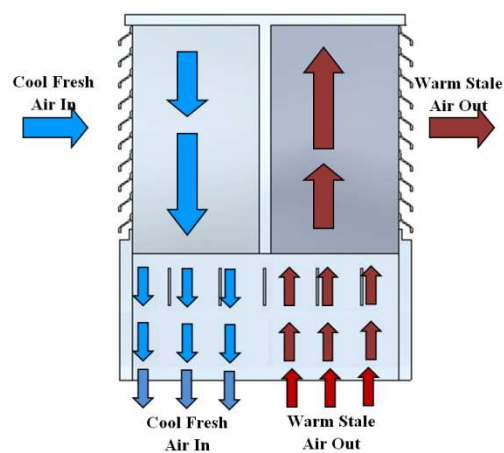


**Figure 1 – Ventilation through a standard commercial wind tower**

To improve the year-round capabilities of wind tower systems to enable consistent use during cooler months, a retrofit heat recovery system is desirable. This study introduces and discusses the potential of this concept through the use of CFD analysis and wind tunnel experimental for validation.

The concept is to attach a rotary thermal wheel to the bottom of a wind tower, as shown in Figure 2. Using the properties of the thermal wheel as a heat exchanger, the thermal energy in the internal exhaust air is recovered to the incoming air. This concept raises the incoming air temperature. By raising the temperature of the incoming air from the wind tower, adequate year round ventilation is maintained and during the heating season, energy demand for heating systems is reduced.

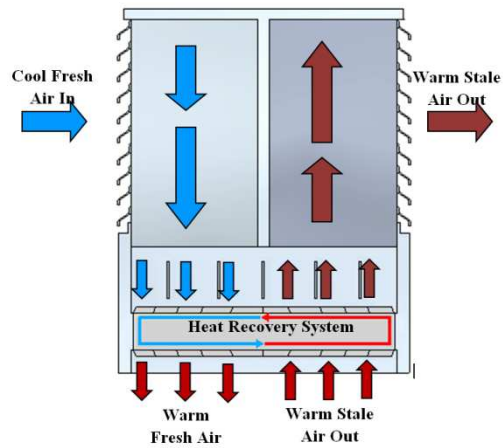


**Figure 2 – Ventilation through the proposed wind tower system with integrated heat recovery technology**

It has been previously noted that wind towers are capable of delivering adequate levels of ventilation, as given in BS5925:1991, to meet pollutant removal guidelines (12); therefore the blockage cause by the rotary thermal wheel must not impede the ventilation rate of the wind tower to a level where these guideline ventilation rates are no longer met.

The two characteristics that were investigated were the flow distribution around the room and the air flow through the four quadrants of wind tower; this was used for the calculation of ventilation supply and exhaust rates. The study shows the inclusion of the rotary thermal wheel will affect the air supply rate into the room/building and determines if the guideline air supply rates are met for standard occupancy. In addition, the potential for heat recovery is analysed with preliminary results presented.

## **2. Previous Related Work**

In recent years, wind towers have undergone considerable amount of research to better understand the effect of airflow through and over wind towers as well as the ventilation rates that can be provided by these systems. Further to this, attempts have been made to improve the thermal comfort that can be provided to occupants, either through the cooling of air for hot climates or warming in cooler climates. The work has been conducted through the use of CFD modelling as well

as scaled wind tunnel testing and in some cases, in situ or field testing in order to understand the effects in a real world environment.

Understanding the ventilation rates through the use of wind towers is essential in encouraging the uptake of the technology for the wider public. In order for this to be successful, research needs to confidently show that acceptable levels of ventilation can be achieved. Hughes & Ghani (13) used CFD analysis to show that wind towers are capable of supplying the recommended air supply rates even at low external wind velocity. This simulation work is supported by in-situ wind tower testing focussed on the ventilation rates that were achievable. Jones & Kirby (8) investigated ventilation rates in schools and saw a 46% increase when a wind tower was used in conjunction with natural ventilation strategies such as opening windows and doors to aid circulation. Kirk & Kolokotroni (14) investigated ventilation rates in office buildings and recorded an increase of 87% in ventilation rates compared to mechanical ventilation when a wind tower was used.

CFD analysis can also be used to determine the most effective configuration of wind towers by analysing the flow effects around the unit. Liu *et al.* (15) found that the optimal number of louvers in the design of a wind tower was found to be between 6 and 8. Beyond this value the airflow rate did not increase by a significant amount to warrant the additional material.

In addition to CFD analysis, scaled wind tunnel testing is essential to gain qualitative and quantitative data from concepts and prototypes in a controlled environment. Wind tunnel testing can be used to validate work previously analysed using CFD models. Walker *et al.* (16) used scaled model testing in wind tunnels to validate CFD models. The results from their data showed high levels of correlations. This shows that when the CFD models are calibrated to best replicate the conditions found in wind tunnels, errors are eliminated. Montazeri *et al.* (17) and Montazeri (18) used wind tunnel testing for the qualitative visualisation of air streams for alternative wind tower shape designs. Testing in this way furthers understanding of the air flow and characteristics through a building model, giving a transient solution that CFD sometimes is not able to replicate. Elmualim (19) showed the use of full

scale models in large wind tunnels has shown positive results and validation of CFD analysis.

However it should be noted that with these tests, atmospheric conditions cannot be replicated in a small wind tunnel as the roof of the wind tunnel will lead to artificial acceleration of the air. Shea *et al.* (20) and Elmualim (21) have conducted far-field testing of wind tower systems in order to determine the suitability of the system outside of a wind tunnel.

Following work investigating the effects of flow around a wind tower, various attempts have been made to enhance the cooling and heating potential of wind towers. Bouchahm *et al.* (6), Bahadori (7) and Bansal *et al.* (22) focussed on the inclusion of additional cooling techniques for wind towers. The work sought to make use of the evaporative cooling technique which was commonly used in the traditional designs to cool the incoming air. Though cooling has had more attention in the past, little work has been carried out in the area of heat recovery or heating incoming air in wind towers. Shao *et al.* (23) noted that passive stack systems are designed without heat recovery which leads to large amounts of wasted heat. Woods *et al.* (24) looked at the use of wind towers during the winter using air mixing techniques to dilute the incoming cool air with the internal air. This system increased the incoming air temperature, thereby negating the heat demand whilst maintaining adequate pollutant levels but required very strict building design and control systems.

Though this area of research is expanding with more teams exploring the potential of heat recovery in passive ventilation systems, little work has been performed on the use of the rotary thermal wheels specifically in natural ventilation. Younis & Shoukry (25) and Calay & Wang (26) examined the use of rotary thermal wheels for residential building applications. These studies indicate that a rotary thermal wheel may be applicable for heat exchange in ventilation, both for summer and winter conditions. However, both studies used forced ventilation in order to overcome the expected pressure drop across the rotary wheel which leads to the energy implication of the fans.

Rotary thermal wheels provide heat recovery at a high efficiency, even when compared to other heat recovery technology. The potential for energy savings through the use of a rotary thermal

wheel coupled with a passive ventilation system such as a wind tower are high. The lack of current research exploring a system similar to this demonstrates a key gap in existing knowledge. This study developed both a CFD model and a 1:10 scaled model for validation using in a wind tunnel to determine the viability of this concept.

### **3. CFD Model Setup**

The CFD code ANSYS Fluent 14 was used to predict the characteristics of the air flow through the wind tower models into the building model. To ensure that the CFD models were accurate and reliable, the parameters and boundary conditions reflected those found in the wind tunnel experiments.

The flow was assumed to be three dimensional, laminar and incompressible. The low Reynolds, laminar nature of the flow was modelled in the CFD software by using the k- $\epsilon$  viscous model with standard wall functions, this is the common method proposed by literature (5, 12, 17-19, 27, 28) with Reynolds numbers in the range of 3000-7500. This technique is also well established in the field of natural ventilation research. However, due to the discrepancy between different sources (19), both the standard and RNG k- $\epsilon$  viscous models were run and compared with the wind tunnel experimental data to find the most applicable solution. The wind tower without the rotary thermal wheel was used to initially compare the different turbulence models. The CFD codes use the Finite Volume Method (FVM) approach and employs the Semi-Implicit Method for Pressure-Linked Equations (SIMPLE) velocity-pressure coupling algorithm with second order upwind discretisation. The governing equations are established and widely used; description and derivations are available in (29) and will not be repeated here.

Geometric computational models were created which exactly replicated the geometric designs of the physical models used in the wind tunnel experiments. The macroclimate domain of the CFD model was designed as the test section of the wind tunnel with dimensions of 500 x 500 and a length

of 1000mm with only the wind tower in the domain; this reflected the experimental model accurately.

The rotary thermal wheel could not be designed in the same manner as the actual physical model; therefore a solid cylindrical volume of the same dimensions was created. The rotation speed and porosity of the rotary thermal wheel was modelled using frame motion and the porous media conditions in ANSYS FLUENT. The frame motion of the flat surfaces of the cylinder was orientated around the central vertical axis of the volume; this ensured that the surfaces rotated around this centre point at the required speed of 150rpm (15.7 rads/s), which is scaled by 10 from the standard rotation speed of 15rpm. Similarity between the scale model and the full size design is recognised using a standard scale of 1:10. To maintain equal conditions between model scale and full scale, similarity analysis was conducted which can be found in Section 4.1.

Porous media settings were applied to the volume of the cylinder. The curved walls of the cylinder did not allow any flow to pass through, matching the wind tunnel model. The porosity of the surfaces was controlled by the inertial resistance equation, (Equation 1).

**Equation 1 (29)**

$$C_2 = \frac{1}{C^2} \frac{\left(\frac{A_p}{A_f}\right)^2 - 1}{t}$$

For a porosity of 70%, the  $C_2$  value for the rotary thermal wheel model was found to be 89.6. Where  $C_2$  is the inertial resistance,  $C$  is the coefficient based on the Reynolds number and  $D/t$ ,  $A_p$  is the total area,  $A_f$  is the free area and  $D/t$  is the hole diameter/plate thickness.

### **3.1.Mesh Generation**

The generation of a high quality mesh is a major factor in the accuracy of results obtained from CFD modelling and the convergence of the model. A non-uniform tetrahedral mesh was applied to a computational model of a wind tower without a rotary thermal wheel. This was done in order to



initially understand the air flow characteristics around the wind tower and building model and how these may be affected by the rotary thermal wheel. Furthermore, an initial design allows for the most acceptable boundary conditions and turbulence models to be tested and applied. This same mesh method was then applied to the wind tower with rotary thermal wheel model.

The geometry for the two models created was very similar. The geometry for the standard wind tower was separated into two different zones; the test section including the wind tower and the building model. The geometry for the wind tower with rotary thermal wheel was separated into three different zones; the test section including the wind tower; the cylindrical volume of the rotary thermal wheel and the building model.

### **3.2.Grid Verification**

The h-p adaption method was used in this study for the mesh created for the standard wind tower and the wind tower with rotary thermal wheel (30). This adaption technique uses high order approximations, measuring accuracy against a user defined indicator between approximations. The entire computational domain was refined from the initial mesh size. The indicator that was used was the average air velocity measured below the wind tower and rotary thermal wheel.

The standard wind tower was meshed using a tetrahedral mesh up to a grid size of 1,149,481. This was done iteratively from an initial size of 67,120 elements to test the grid independency of the model, see Figure 3. The same method was used for the wind tower with rotary thermal wheel mesh generation. The standard wind tower model was shown to be grid independent; the average air velocity measured in the four quadrants of the wind tower was consistent across the final two meshes meaning that the penultimate mesh gave acceptably accurate data.

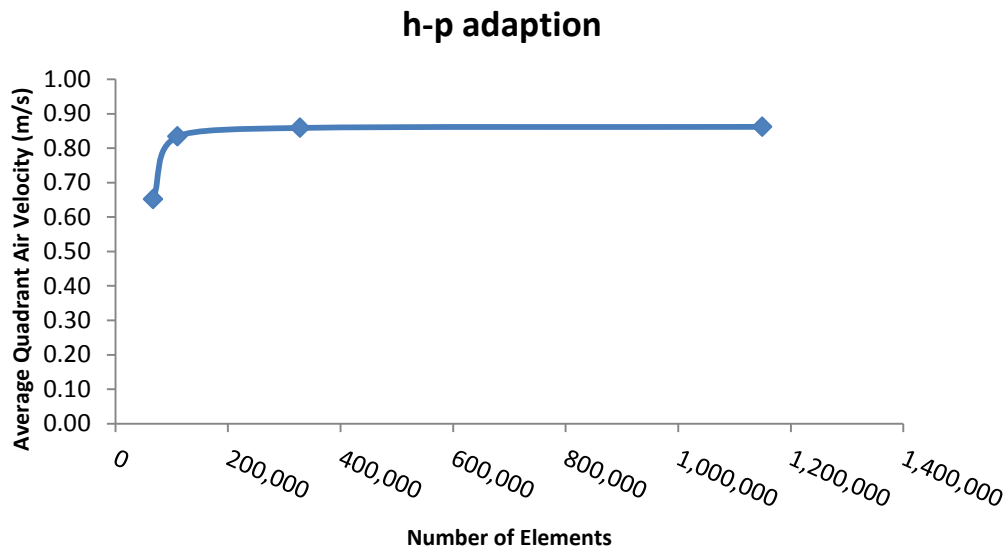


**Figure 3 – Grid independence test of average quadrant air velocity of standard wind tower model over increasing mesh size**

For the wind tower with rotary thermal wheel, the mesh element size was reduced, increasing the number of cells in the domain. A maximum grid size of 2,703,846 was created, an increase of 2,627,267 cells from the initial mesh. . The refinement of the last two stages of the mesh gave a consistent value of average velocity measured within the quadrants of the wind tower. This is shown in Figure 4. This confirmed that the model is grid and mesh independent and capable of delivering acceptable accuracy for data measurement (5).

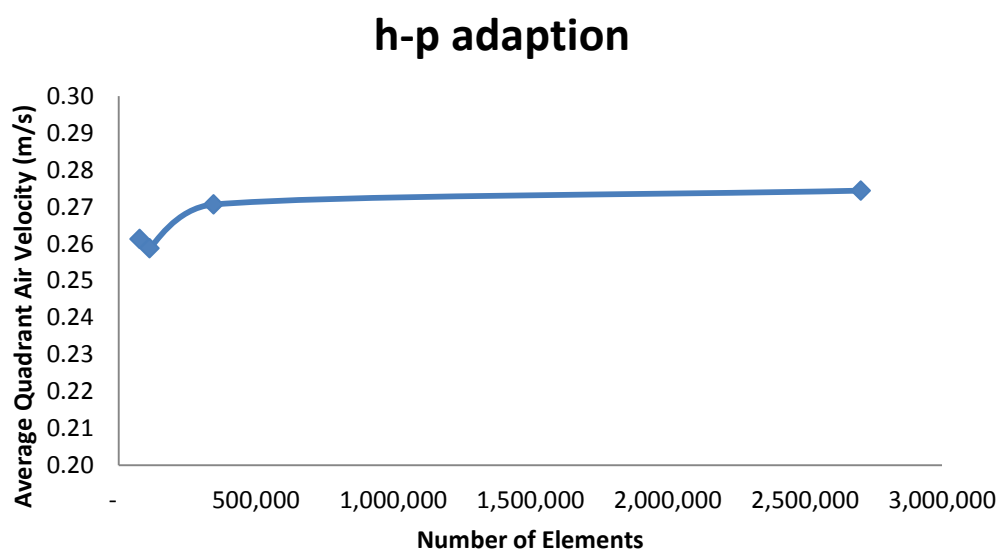


**Figure 4 – Grid independence test of average quadrant air velocity over increasing mesh size**

### 3.3. Boundary Conditions

The boundary conditions for the CFD analysis were governed by the k- $\epsilon$  model. It has previously been shown that the RNG k- $\epsilon$  model is the most applicable in building ventilation models (28, 31). However, other work shows that for low inlet air velocity simulations, the standard k- $\epsilon$  model is more suitable. A comparison between these two viscous models was undertaken to determine which was the most accurate for this situation with respect to the data produced from the experimental wind tunnel tests. Standard wall functions were applied for each viscous model (17-19).

In comparison with the wind tunnel experiments the standard k- $\epsilon$  model gave data with a lower percentage error than the RNG k- $\epsilon$  model for the average indoor air velocity measured. The average error between this model and the experimental data was 30.58% whereas the RNG turbulence model was 55.39%. This correlates with data given in previous literature (17-19, 28, 31).

In the CFD model, inlet conditions were used that would best replicate those in the wind tunnel. The inlet velocity profile was uniform across the height of the test section for both the CFD model and the wind tunnel experiment. A summary of the boundary conditions can be seen in Table 1.

Table 1 – Summary of CFD Model Boundary Conditions (5, 12, 17-19)

Boundary Condition	Type/Value
Discretisation Scheme	Second Order Upwind
Time	Steady State
Turbulence Model	k- $\epsilon$
Velocity inlet (m/s)	3 - 10
Pressure Outlet	Atmospheric
Gravity (m/s <sup>2</sup> )	-9.81
Wheel Porosity	70%
Wheel Rotation	150rpm
Heat Flux (W/m <sup>2</sup> )	24

Thermal conditions for the floor of the building model were set at a constant heat flux of 24W/m<sup>2</sup>.

This was done to simulate an average value set for heat flux from human occupants in a sedentary state, office work or occupants in a classroom. This methodology has previously been explored and showed positive results in comparison to the experimental wind tunnel model (16). Due to

limitations of the wind tunnel used in these tests, thermal conditions could not be applied. Scaling of temperature would require high temperature levels to be attained which would not be feasible or safe.

The conservation of the Navier-Stokes equations regarding velocity, pressure and thermal energy state that if one characteristic is validated between the CFD model and the experimental model, the two remaining characteristics will be valid. Further, the simple algorithm relies on resolution of pressure and velocity, thus these two parameters were validated experimentally. Therefore, thermal conditions were set to the CFD model only. Validation between the CFD model and experimental model was conducted using the air velocity within the building model.

## **4. Experimental Setup**

### **4.1. Similarity Analysis**

As a reduced scale wind tower was required to fit inside the wind tunnel, similarity analysis was necessary in order to calculate the appropriate working scale with reference to the parameters. Similarity analysis is commonly used to correctly identify the parameters which must be maintained or scaled and has been used in reducing the scale of a prototype building whilst using air as the working fluid (32).

The similarities that should be maintained between full scale analysis and reduced scale models are geometric, kinematic and thermal (16). Geometric similarity can easily be achieved; dimensions are equally scaled down by the appropriate factor. The 1:10 scale used in this work was easily achieved. The case for thermal similarity in this model is discussed in Section 3.3.

To help maintain dynamic flow similarity, the dimensionless force ratios should be kept constant between the full scale and model scale. The Reynolds number is the ratio between the inertial forces and viscous forces; this should be kept the same for both models (33). However, it has been noted

that this is impossible to achieve when using air as the working fluid (4). Elsewhere it is stated that flow in a fully developed turbulent region is independent of the Reynolds number, this can be ensured as long as the critical Reynolds number is exceeded (34).

The value of the critical Reynolds number is difficult to determine due to varying conditions but literature generally shows that fully developed turbulent flow is seen in values above 7500 (35-41). Using the critical Reynolds value of 7500, a scale above 1:60 would be sufficient for this wind tunnel experiment.

## **4.2.Wind Tunnel Model Design**

A 1:10 scaled building model was used to test the air flow characteristics of the wind tower incorporating the rotary thermal wheel model. The model was a cuboid shape, where the only opening was at the ceiling to allow for the wind tower to be attached. The decision not to include any other openings was taken to prevent other ventilation effects disrupting the air flow and introducing inconsistencies into the results. The experiment was conducted in the University of Leeds low speed closed circuit wind tunnel (42).

The wind tunnel used for experimental analysis consisted of an overall plan length of 5.6m with a test section of the height, width, and length of 500, 500, and 1000mm respectively. The tunnel operates as closed circuit or return flow; air that passes through the test section is drawn back into the fan and recirculated into the test section repeatedly. This can lead to the air temperature inside the wind tunnel increasing due to friction and radiated heat from the fan hence, before any measurements were taken, the temperature within the wind tunnel was allowed to normalise. Guide vanes are used to turn the air flow around the corners of the wind tunnel while minimising the turbulence and power loss. The contraction, diffuser, test section and two corners are located at floor level and the return legs set with the axial fan are positioned vertically above the test section, see Figure 5. A similar wind tunnel configuration has been used for experimental analysis of wind towers in previous work (17, 18).

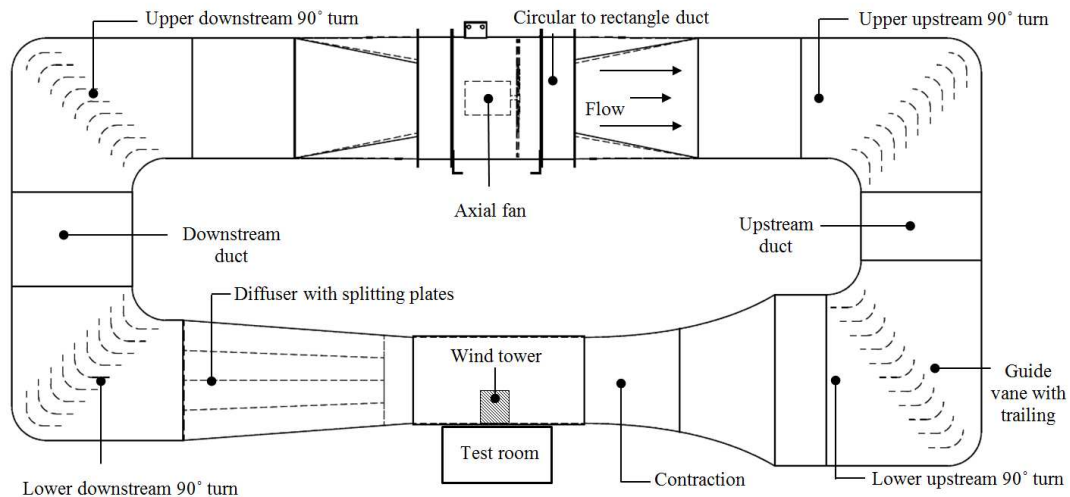


**Figure 5 – Cross section of the closed-loop subsonic wind tunnel facility for investigating the ventilation performance of the wind tower device with rotary thermal wheel**

The 1:10 building model, as seen in Figure 6, was of dimensions 500 x 500 x 270 mm with a 113 x 113 mm square hole in the ceiling where the wind tower was mounted. The wind tower that was used in the wind tunnel experiments was designed as individual components which allowed for the same major components to be interchanged between models. In order to the model to be analysed in the wind tunnel, a scale of 1:10 was determined to be the most acceptable when considering similarity analysis and the physical space limitations of the wind tunnel test section. The dimensions of the wind tower were 113 x 113 x 113mm due to the additional material thickness.

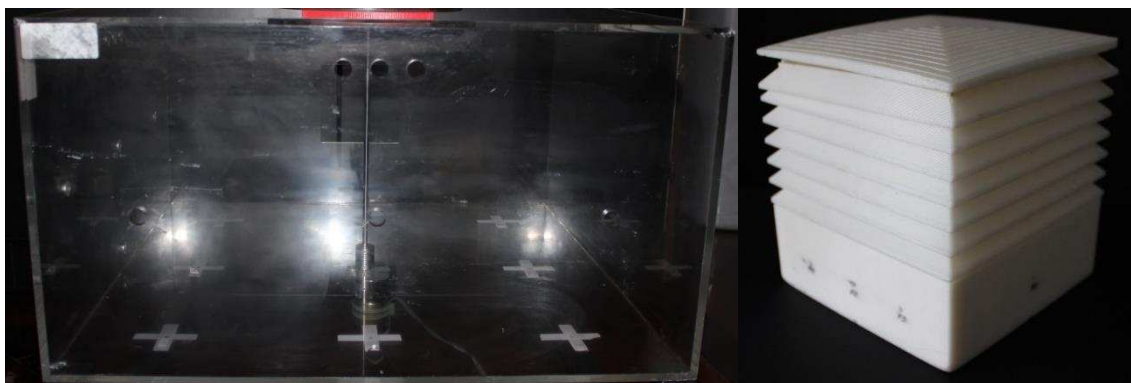


**Figure 6 –Building model (left) and standard wind tower (right) used in wind tunnel experiments. Exact copies were produced for use in CFD analysis**

The thermal properties and characteristics of the rotary thermal wheel could not be replicated at a reduced scale, as such it was deemed appropriate that the air flow characteristics were the most essential to be replicated. To achieve this geometry, porosity and rotation speed were the three

properties of the rotary thermal wheel that were simulated to meet the experimental model scale requirements.

To meet the scale of 1:10, the rotary thermal wheel was designed to be 80mm in diameter with a depth of 20mm. Though the porosity of rotary thermal wheels is commonly as high as 90% (43), it was not possible to reproduce this level of porosity due to the technical limitations and design tolerance of the 3D printer used. A porosity of 70% was used in the final wind tunnel experiments, see Figure 7 .

The rotation speed of a rotary thermal wheel can be varied between 10-15 rpm depending on the conditions. As the purpose of the study was to understand how the air flow characteristics through a wind tower are affected by a rotary thermal wheel, the rotation speed was set to maximum. This created the highest level of blockage for the air to pass through, making this a conservative approach to take. The rotation speed of the model was 150 rpm to conform to the 1:10 scale.

The rotary thermal wheel was held in place in the casing by using supports which did not interfere with the rotation. In order to achieve the required rotation speed for the wheel, a rotation shaft was fitted through the test section vertically which connected to a DC motor underneath the test section as seen in Figure 7. Full sized rotary thermal wheels are belt driven within the casing, however as it was not feasible to create this mechanism for the scale model, alterations had to be made. The rotation shaft was kept as thin as possible in order to prevent the flow being affected. Additionally, measurements were taken at four points around the shaft and averaged in order to determine the air velocity at that point.

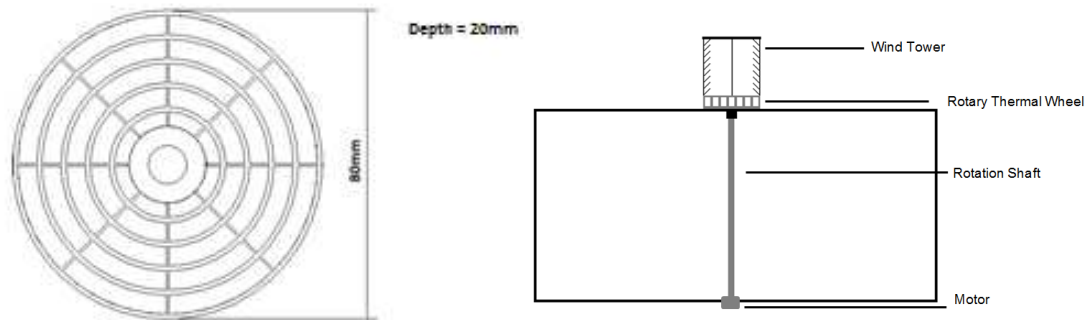


**Figure 7 – Top down view of the rotary thermal wheel model created for use in the wind tunnel experiments (left). A solid volume of the same dimensions was created for the CFD model. Schematic drawing of wind tunnel model design showing rotation shaft connection.**

The rotary thermal wheel model was held in a casing which connected to the building model below and the wind tower above (Figure 8). The additional height of the wind tower which the casing provided had to remain consistent with the standard wind tower model; this was achieved by the addition of an empty casing of the same dimensions, ensuring that both models were held at the same height.



**Figure 8 –Designs of the different casings used to maintain the wind tower height for testing. The standard wind tower casing (left) raised the height of the wind tower to match the height of the wind tower with rotary thermal wheel casing (right)**

### **4.3.Wind Tunnel Measurement Setup**

The test section in the wind tunnel measures 500 x 500 x 1000 mm. In order to accommodate the model and wind tower models, a square section was cut out of the test section which the wind tower models would fit through and attach to the building model below. The height, and thus the blockage ratio, of both wind towers were maintained through the use of casings. The blockage ratio



of the wind tower models in the test section was 5.11%, this is in line with the values recommended in literature (17, 44, 45).

In order to assess the air flow characteristics through the standard wind tower and the wind tower with the rotary thermal wheel, nine predetermined points within the room model and sixteen predetermined points beneath the wind tower quadrants were used for the measurement of the air velocity, see Figure 9 and Figure 10. The nine points within the room model were chosen in order to give an equal spread of measurement points and to ensure that the mixture profile of the air could be monitored (Table 2). All the points were equidistance from each other and the walls of the room model. The sixteen points below the wind tower quadrants were chosen to give an average air flow through the quadrants. A hot wire anemometer measured the velocity of the air in the X, Y and Z directions at three different external wind velocities for both the standard wind tower and the wind tower with the rotary thermal wheel. Before any measurements were taken in the wind tunnel using the hot-wire anemometer, the temperature of the internal air was allowed to normalise to  $23^{\circ}\text{C} \pm 0.2$  due to friction before measurement began.

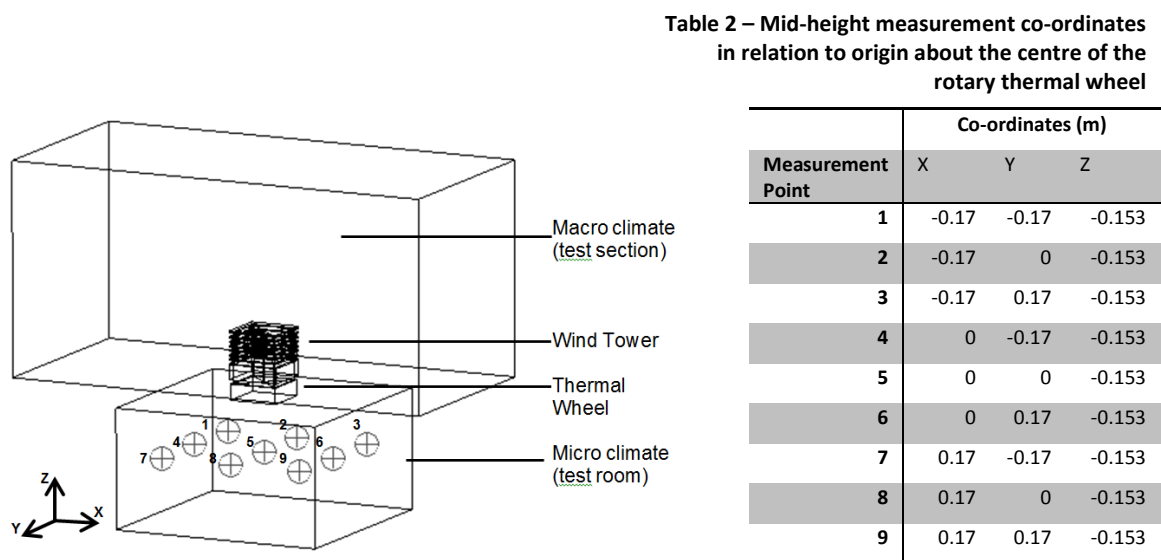


**Figure 9 – Location of the nine measurement points at mid-height of the building model used for the reading of velocity measurements in both the CFD analysis and the wind tunnel experiments**

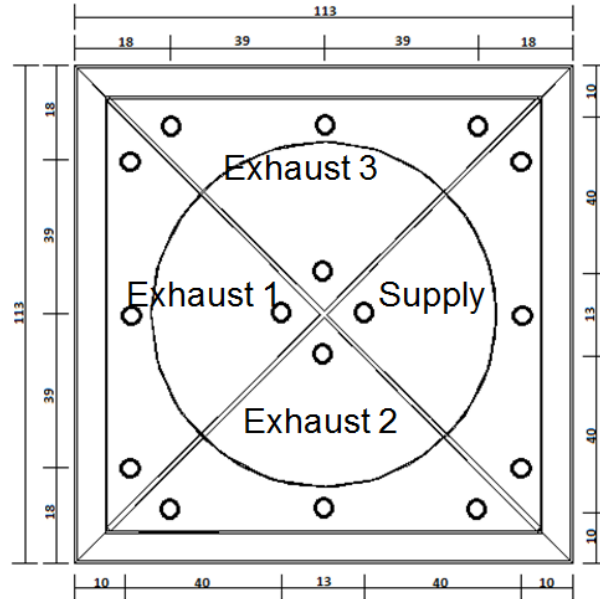


**Figure 10 – Location of the sixteen measurement points below the four quadrants of the wind tower used for the reading of velocity measurements in both the CFD analysis and the wind tunnel experiments. Supply and exhaust conditions of the wind tower are also shown.**

The uncertainties associated with the velocity readings can be determined for the hot wire probe, the hot wire probe (Testo 425) gave velocity measurements with uncertainty of  $\pm 1.0\%$  rdg. at speeds lower than 8 m/s and uncertainty of  $\pm 0.5\%$  rdg. at higher speeds (8 – 20 m/s). The valid angle range for the hot-wire anemometer is within the range of  $\pm 20^\circ$ .

## 5. Validation

To validate the CFD model against the wind tunnel model, the percentage error between the two data sets must be to an acceptable level. In addition to percentage error as an indicator of correlation, identifying equal trends in both sets of data is important to validate the CFD model. To determine the accuracy of the CFD model in relation to the wind tunnel model, first a comparison of the quantitative data was taken to calculate the numerical accuracy. From this, the graphical output from the CFD model was analysed to examine the trends of the data.

The air velocity at the building model mid-height was calculated at each of the nine measurement points for the three different external air velocities. The air velocity underneath the four quadrants of the wind tower was measured at sixteen different points, four per quadrant. From this the air

supply rate can be calculated and scaled up for a full sized wind tower and room. These measurement points were replicated in the CFD model.

Table 3 shows the measurement of air velocity at the nine measurement points around the building model at three different inlet air velocities for both the CFD analysis and the experimental wind tunnel test. The average percentage error between the experimental wind tunnel test and the CFD analysis is consistent. At 3m/s the percentage error is marginally lower than the values seen for 6m/s and 10m/s. It can be seen from the table that the error at a number of points is larger than that at other points. The inconsistencies at point 2, 4, 7 and 9 are significantly higher than those at the remaining points. Though there is no pattern that can be identified from the location of these points relative to the building model geometry or location in the building model, other explanations of the error may be possible. Errors within the CFD mesh close to these points would have a significant follow on effect on the air flow measured. The use of the standard  $k-\epsilon$  equation cannot accurately model recirculation that occurs within the building model (46). The recirculation area is frequently overestimated which will lead to incorrect results as demonstrated by the inconsistencies.

**Table 3 – Comparison and percentage error calculation of air velocity measured from CFD analysis and wind tunnel experimental testing at nine measurement points over three different inlet velocities.**

Air Velocity									
	3m/s			6m/s			10m/s		
	CFD (m/s)	Experiment (m/s)	% Error	CFD (m/s)	Experiment (m/s)	% Error	CFD (m/s)	Experiment (m/s)	% Error
Point 1	0.12	0.15	16.31	0.24	0.32	25.16	0.38	0.44	13.71
Point 2	0.06	0.12	54.23	0.10	0.23	55.50	0.18	0.43	57.28
Point 3	0.11	0.13	17.00	0.19	0.31	38.79	0.30	0.36	17.31
Point 4	0.05	0.10	47.79	0.14	0.27	48.70	0.26	0.40	35.00
Point 5	0.59	0.84	29.89	1.35	2.05	34.10	2.16	3.27	33.89
Point 6	0.10	0.14	29.80	0.22	0.36	40.60	0.37	0.62	40.75
Point 7	0.10	0.19	46.52	0.21	0.40	46.47	0.33	0.54	39.62
Point 8	0.06	0.08	26.06	0.13	0.15	16.76	0.15	0.42	65.41
Point 9	0.07	0.13	43.26	0.17	0.31	44.04	0.29	0.47	39.45
	Average Error		34.54	Average Error		38.90	Average Error		38.05

As can be seen from Figure 11, the CFD analysis consistently underestimates the internal air velocity compared to the values measured from the wind tunnel tests. This is significant in the development

of future models and the appropriate selection of turbulence models used in CFD analysis as discussed above. Furthermore, the boundary conditions in the CFD model were kept as similar as possible to those in the experiment, minimising the error which could be caused. Grid independency was undertaken and showed the mesh was good quality. Underestimating the air velocity introduces subsequent error for further analysis of the experiment and viability of the system.

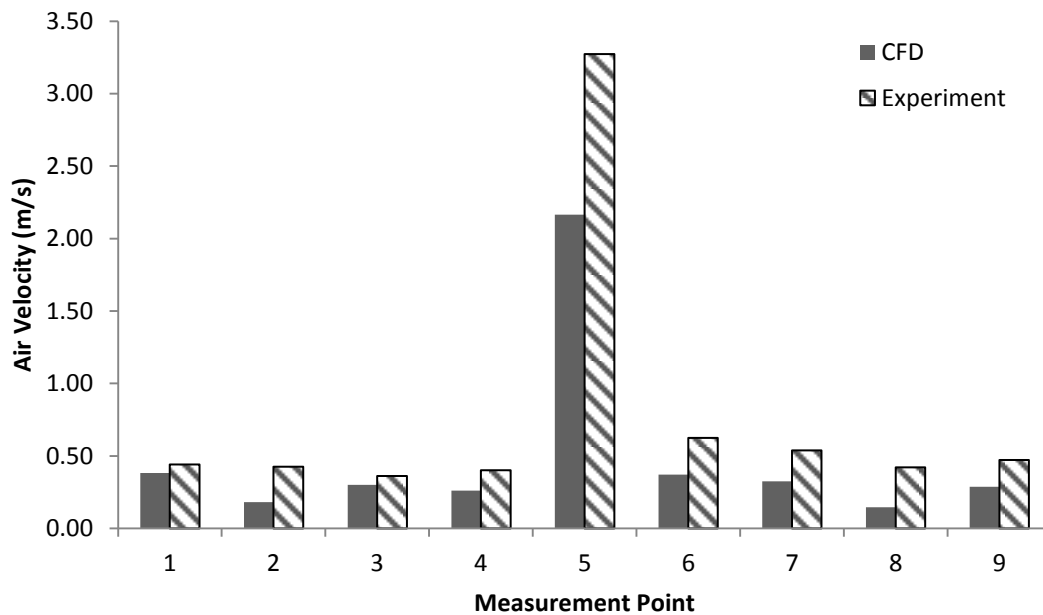


**Figure 11 - Comparison of Air Velocity at Nine Measurement Points between CFD Analysis and Experimental Wind Tunnel Testing**

Though the CFD model consistently underestimates the air velocity at the nine measurement points compared to the experimental models, the same distribution of air velocity can be identified. The similar trends of air velocity for both data sets show that the CFD model is validated by the experimental wind tunnel testing.

## 6. Results and Discussion

The main focus of this study was to compare the results of air flow characteristic analysis from the wind tunnel experimental model of a wind tower with rotary thermal wheel with the results from

CFD analysis. Three cases were compared for the wind tower with rotary thermal wheel, where the external air velocity was 3, 6 and 10m/s.

The air velocities within the building model were measured at mid-height of the building model and below the four quadrants of the wind tower. The measurement of the air velocity below the quadrants was done in order to calculate the air supply rates and determine whether the guidelines levels could be met by the wind tower with rotary thermal wheel system.

## 6.1. Indoor Air Velocities and Patterns

The air pattern inside the building model gives an indication of the circulation of the incoming air into the building model, this is important in determining whether the inclusion of the rotary thermal has a significant negative effect on the air flow into the building model compared to the standard wind tower. Understanding how the rotary thermal wheel affects the flow of air through the wind tower into the building is essential in order to develop the system and identify its limitations.

As can be seen in Figure 12, there is a significant amount of air distribution around the building model away from the inlet quadrant of the wind tower. This suggests that the incoming air will be well distributed to all areas of the building, ensuring that fresh air can be introduced to all occupants. The ability for air distribution is further highlighted in Figure 13, showing the air velocity contour at mid-height of the building model.

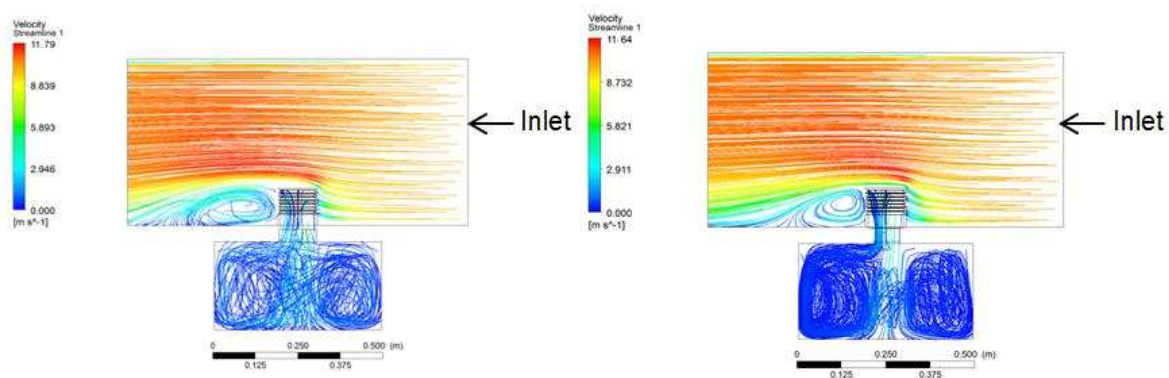
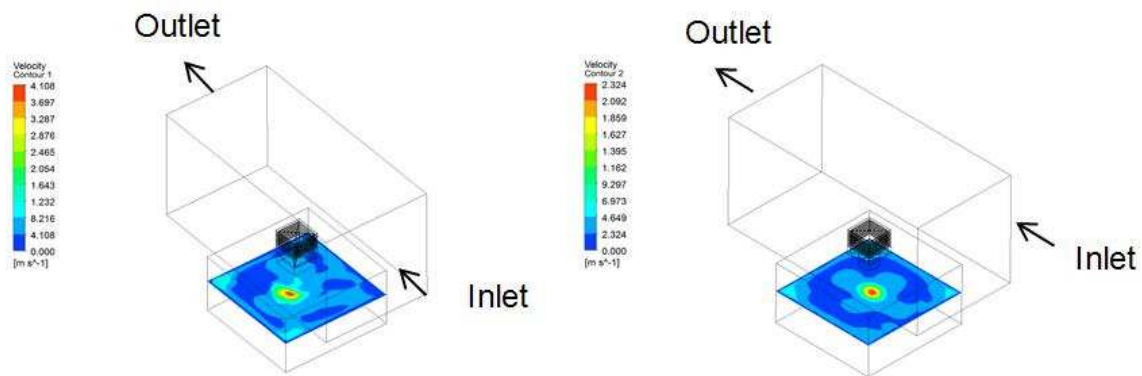


Figure 12 – Streamline analysis of wind tower (left) and wind tower with rotary thermal wheel (right) rotating at 150rpm with an inlet air velocity of 10m/s



**Figure 13 – Horizontal contour plot of air velocity at building model mid-height showing the distribution of air velocity inside the building model, wind tower (left) and wind tower with rotary thermal wheel (right)**

## 6.2. Air Supply Rates

A key area to test the suitability of the wind tower with rotary thermal wheel in a realistic environment was to determine the air supply rate of the system. By calculating the air supply rate of the system under a range of inlet air velocities the ventilation rates for a set occupancy was determined. The air supply rate was calculated by using the air velocity in the supply quadrant of the wind tower, the value of this can be seen in Table 4. The percentage error between the CFD analysis and the experimental wind tunnel testing was significantly smaller than the error seen at the nine measurement points at the building model mid-height.

**Table 4 – Comparison and percentage error calculation of air velocity measured from CFD analysis and wind tunnel experimental testing in the four quadrants of the wind tower with rotary thermal wheel over three different inlet velocities.**

Velocity (m/s)	3m/s			6m/s			10m/s		
	CFD (m/s)	Experiment (m/s)	% Error	CFD (m/s)	Experiment (m/s)	% Error	CFD (m/s)	Experiment (m/s)	% Error
Supply	0.47	0.54	13.62	0.93	1.23	24.85	4.58	5.93	22.77
Exhaust 1	0.21	0.24	9.57	0.41	0.48	13.84	2.06	1.46	41.10
Exhaust 2	0.19	0.19	1.76	0.37	0.35	7.45	1.60	1.42	12.68
Exhaust 3	0.21	0.19	10.39	0.37	0.38	0.67	1.60	1.41	13.21
	Average		8.84	Average		11.70	Average		22.44

To calculate the air supply rate, the volume of air moving into the room model was determined from air velocity at the supply quadrant of the wind tower multiplied by the area of the quadrant. This value was then converted into litres per second. The air supply rates, as seen in Table 5, are in agreement to those published in previous work (5). Though there is similarity between existing air

supply rates for wind towers and the air supply rates calculated, the addition of the rotary thermal wheel caused a noticeable reduction in the supply rate, see Figure 14.

The errors that can be identified in both Table 4 and Table 5 are due to the limitations of the standard k- $\epsilon$  equation used for turbulence modelling. Because of the rotating mesh used to model the rotary thermal wheel, complex flows are created below the wheel. The swirling effect below the wheel is difficult to model using the standard k- $\epsilon$  equation and causes high levels of error.

In Table 4, the greatest error between the CFD data and the experiment data for the 3 and 6m/s inlet velocity scenarios is in the inlet quadrant, 13.68% and 24.85% respectively. This is due to the increased volume of air that flows through a single quadrant compared to the three exhaust quadrants which have lower volume of air. However, in the case of 10m/s inlet velocity, exhaust 1 has a significantly higher error than the supply quadrant and the remaining exhaust quadrants, 41.10% compared to 22.77%. The increased air inlet velocity and rotating mesh used in the model may create additional error. Further investigation is needed with regard to this error in exhaust 1.

In Table 5, the difference between the air supply rates in the CFD results and the experiment results is greater at each inlet velocity for the supply quadrant of the wind tower. At 10m/s the error is significantly larger for all quadrants than that for the other inlet velocities. The instantaneous exchange of indoor and outdoor air is cancelled out by the averaging method of calculating air flow. This results in lower ventilation rates and air change effectiveness (47). As the inlet air is at a greater velocity, the error will be increased compared to the lower inlet air velocities.

**Table 5 – Comparison of air supply rates based on CFD analysis and wind tunnel testing for full scale wind tower designs.**

	3m/s		6m/s		10m/s	
	CFD (L/s)	Experiment (L/s)	CFD (L/s)	Experiment (L/s)	CFD (L/s)	Experiment (L/s)
<b>Supply</b>	108.35	125.32	216.11	287.31	458.00	593.00
<b>Exhaust 1</b>	49.51	54.71	95.53	110.77	206.00	146.00
<b>Exhaust 2</b>	44.85	44.04	86.79	80.70	160.00	142.00
<b>Exhaust 3</b>	49.51	44.81	86.79	87.30	160.00	141.33

A standard occupancy density for schools and offices has previously been determined (11). Both these values were used in determining the air supply rate per person of the building model used in this study as the dominate consumers of wind tower products. The required air supply rate to meet guideline ventilation levels for both schools and offices is 8L/s per person (48, 49). Based on these required values of ventilation, the wind tower with rotary thermal wheel is capable of meeting these guideline levels above an inlet air velocity of 3m/s for 13 occupants in a school and 2 occupants in an office. Below this inlet air velocity, the ventilation guidelines would not be met for the school room. It should be noted that the average wind speed above 25m in the UK is greater than 5m/s (50). This value is above the 3m/s inlet velocity and so suggests that the wind tower with rotary thermal wheel would be capable of meeting the ventilation requirements much of the time. Below 3m/s inlet air velocity, the required ventilation rates can still be met for rooms with lower occupancy. Figure 14 compares the guideline air supply rate per person against the air supply rate per person calculated for a wind tower and a wind tower with rotary thermal wheel using both experimental and CFD data. At air velocities 5m/s and above, all of the configurations exceed the guideline levels of air supply rate per person.

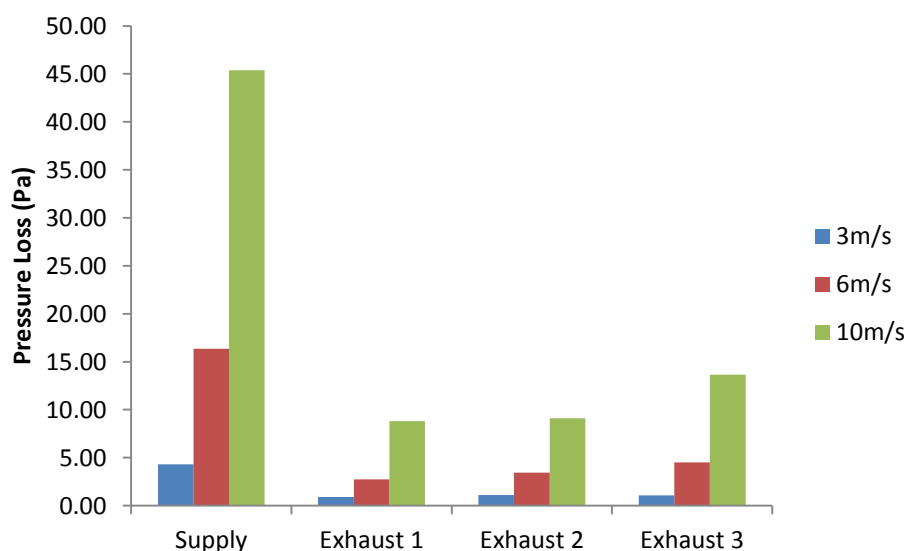


**Figure 14 – Comparison of air supply rate for a wind tower and a wind tower with a rotary thermal wheel against the guideline supply rate of 8m/s.**



The results shown in Table 6 can be compared to data obtained in previous work from a study on the ventilation rates in a number of school classrooms (10). Two of the eighteen classrooms studied were naturally ventilated using wind tower systems. The classrooms were normalised for occupancy and volume to ensure that a fair comparison could be made. It was noted that during the winter months that six of the classrooms were not capable of meeting the minimum ventilation rate at any time of 3L/s/p but the classrooms ventilated using the wind tower may be capable of reaching these guideline levels if better designed.

**Table 6 – Calculation of air supply rate per person for standard occupancy densities as determined previously for both school classrooms and office spaces. 1) Calculation of supply rate for a wind tower with rotary thermal wheel. 2) Calculation of supply rate for a wind tower.**

Supply Rate per Person (10)				Supply Rate per Person					
				3m/s		6m/s		10m/s	
				CFD (L/s/p)	Experiment (L/s/p)	CFD (L/s/p)	Experiment (L/s/p)	CFD (L/s/p)	Experiment (L/s/p)
	Occupant Density (m <sup>2</sup> /person)	Number of Occupants	Required Supply Rate (L/s/p)						
1) School	1.8	13.9	8	7.80	9.02	15.56	20.69	32.98	42.70
Office	10	2.5	8	43.34	50.13	86.44	114.93	183.20	237.20
2) School	1.8	13.9	8	22.63	27.66	39.64	56.40	133.59	125.71
Office	10	2.5	8	125.71	153.65	220.23	313.35	742.17	698.40

For occupancy of 10 and 15 for the two classrooms using wind tower systems, the “usual” ventilation rate was 5.5L/s/p and 3.4L/s/p respectively. These values are lower than the values calculated for classroom occupancy of 13.9 in the model for both the CFD analysis and the experimental wind tunnel testing. As the measurements of 5.5L/s/p and 3.4L/s/p are taking from onsite readings, it can be presumed that the data is accurate, though no measurement of external wind velocity is given for these ventilation rates which may explain the low values.

### 6.3. Pressure Drop across Rotary Thermal Wheel

The pressure drop across the rotary thermal wheel was measured in the CFD model. Measurements were taken directly above and below the rotary thermal wheel and an average pressure drop was calculated for each quadrant. As expected, the pressure drop increased across all four quadrants of the wind tower as the external air velocity increased, as seen in Figure 15. Furthermore, the supply quadrant consistently measured a higher pressure loss than the three exhaust quadrants. This is due

to the increased volume of air which will be moving through the supply quadrant compared to the three exhaust quadrants.

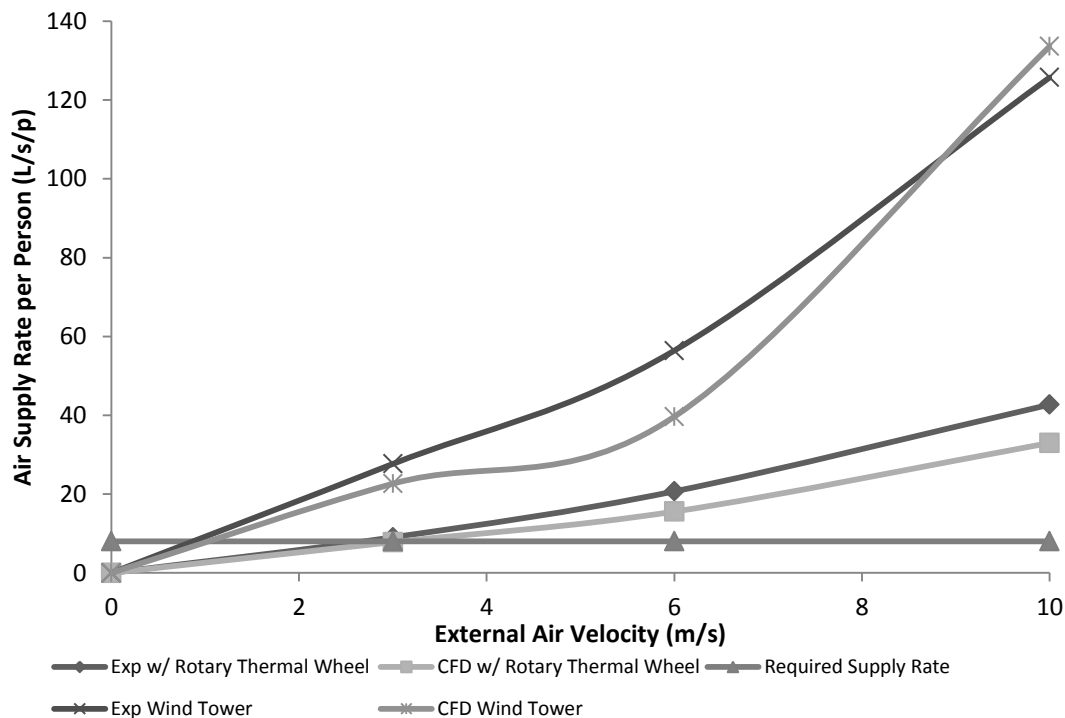


**Figure 15 – Pressure drop across the rotary thermal wheel measured at three inlet air velocities**

The maximum pressure loss across the heat exchanger was 45.40Pa in the supply quadrant at 10m/s inlet air velocity. Though this is a significant loss, previous results show that the airflow rate into the building model is not affected in a noteworthy way. Moreover, work has previously been conducted using a wind tower integrated with a fixed plate heat exchanger which showed a similar pressure drop across the heat exchanger. At an inlet air velocity of 3.1m/s, a pressure drop of 30Pa was measured which is significantly higher than the pressure loss measured in this work (51). At a similar inlet air velocity, the maximum pressure loss was measured as 4.33Pa. This suggests that the rotary thermal wheel is a more suitable heat recovery device for integration into a commercial wind tower system.

## 6.4. Internal Air Temperature

The internal air temperatures were measured at the same nine measurement points that were used for the air velocity over three different inlet velocities. A number of trends can immediately be

identified from Figure 16. As expected, the internal temperature falls as the inlet velocity increases. What is noticeable is the rate at which the internal temperature falls as the inlet velocity increases. From 3m/s to 6m/s external wind speed, a more substantial temperature drop is seen than from 6m/s to 10m/s. This is likely due to the equalising of the temperature of the inlet air with the internal heat flux. The inlet air temperature was set at 296.19K (23.2°C), matching the temperature measured in the wind tunnel.

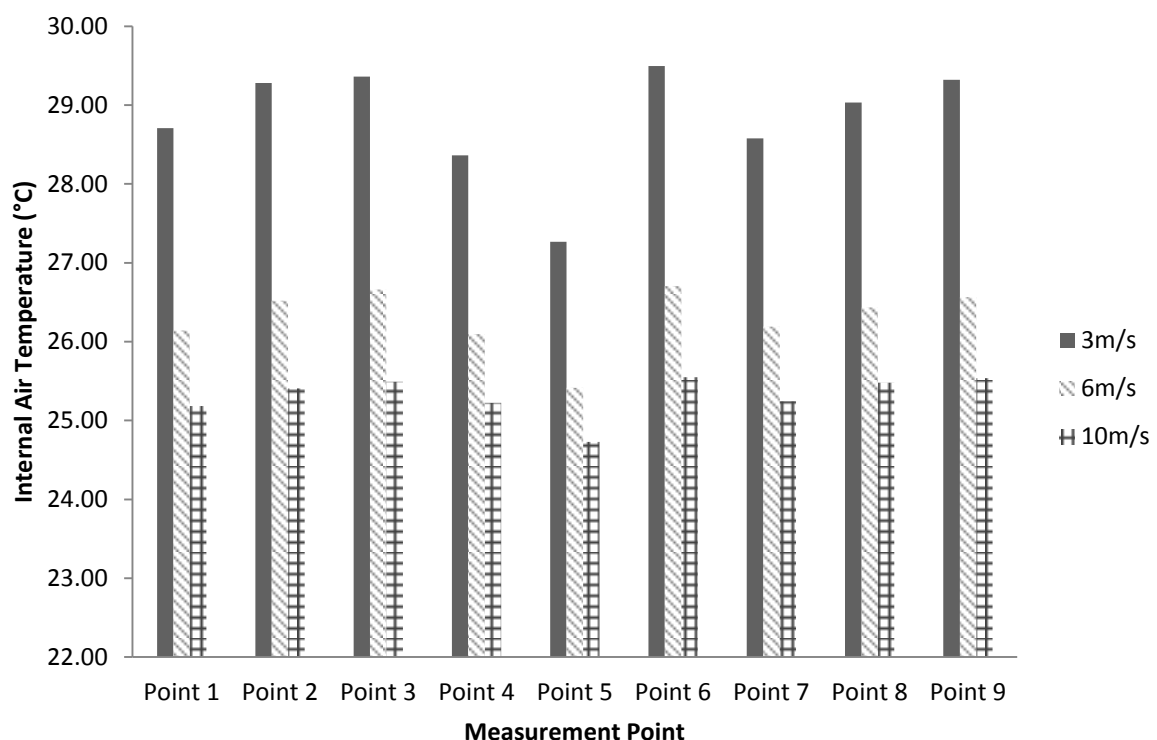


**Figure 16 – Comparison of internal air temperature measurements at three inlet air velocities taken from CFD simulations using a heat flux of 24W/m<sup>2</sup> applied to the floor area.**

A second observation is the distribution of the heat across the building model. Point 5 is directly beneath the wind tower; as such the incoming air temperature has a significant effect, making the temperature at this point approximately 1.5°C lower than the average temperature across the nine measurement points at an inlet speed of 3m/s, this falls to 0.5°C lower than the average temperature at 10m/s.

The points within the building model downwind of the inlet show a lower temperature than those upwind. This is due to the direction of the cooler inlet air temperature moving into the building

along with the effect of pressure on the leeward side of the wind tower and building, drawing air from the building.

It is worthy to note the temperature difference seen in the cylindrical volume of the rotary thermal wheel. On the inlet stream of the wheel, the air temperature is at 23.2°C. On the outlet stream of the wheel, the air temperature is 25.2°C due to the heating effect of the floor area. This suggests that if the increased temperature in the outlet stream can be recovered and transferred to the inlet stream, the inlet temperature would reduce the demand on any heating system used. Further to this, the inlet air temperature was set at 23.2°C which is higher than average outdoor air temperature recorded in the UK between 1981 and 2010 of 12.4°C (52), meaning that the outlet stream temperature would be significantly higher than the inlet stream temperature, giving great potential for thermal energy recovery and transfer.

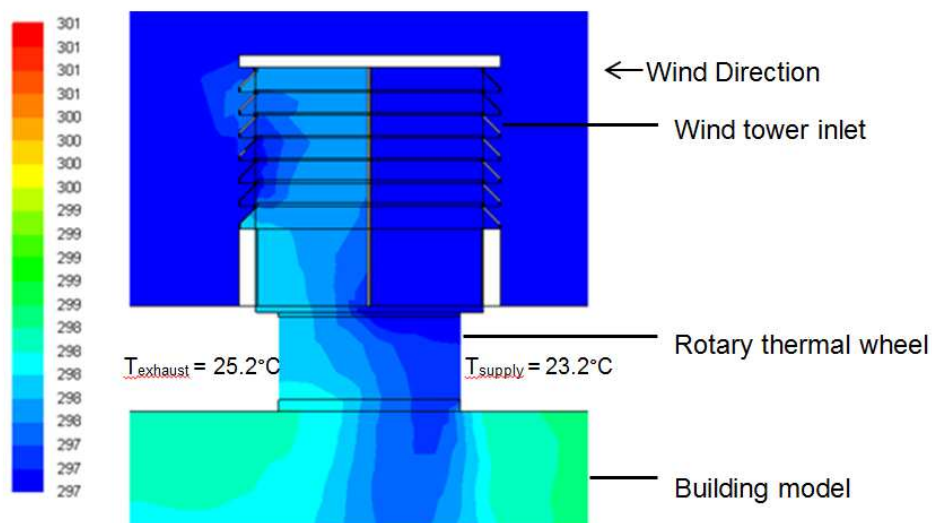


Figure 17 – Temperature contour across the wind tower and rotary thermal wheel at an inlet velocity of 10m/s with inlet temperature of 23.2°C (296.2K).

## 7. Conclusion

The aim of this study was to determine whether the air flow through a wind tower is significantly affected by the inclusion of a rotary thermal wheel at the base of the wind tower. It has been shown in previous work that wind towers are capable of delivering the guideline levels of ventilation into a

room, therefore the rotary thermal wheel should not reduce the air supply rate to unsuitable levels to provide adequate ventilation to be an effective system. CFD models were validated against experimental models tested in a closed circuit wind tunnel for a wind tower concept that incorporated a rotary thermal wheel in the structure.

The comparison between the CFD and experimental model showed a strong correlation between the two sets of data. Though an error between the CFD and experimental results of approximately 36% existed, the same trend of the air velocity within the building model can be identified in both the CFD and experimental data. It has previously been noted in literature that in the study of natural ventilation effects, errors up to 100% between CFD and experimental models can be deemed acceptable when positive trends between the two sets of data can be observed (27, 53).

In order to determine whether the rotary thermal wheel impeded the air supply rate into the building model, the air supply rate was investigated and compared both to existing guideline values and previous work. The wind tower with rotary thermal wheel was capable of meeting the guideline ventilation rates above an inlet air velocity of 3m/s for a standard occupancy density of 1.8m<sup>2</sup> per person. Below this inlet air velocity it is unlikely that ventilation would be adequate for a classroom with 13 or more occupants. It should be noted that a value of 1.8m<sup>2</sup> per person is the minimum value for occupancy density in a classroom, as this value increases it is possible that the ventilation rates would be suitable for the reduced number of people. By comparing the results of the air supply rate from the wind tower with rotary thermal wheel to previous work, although the air supply rates did not match, the values exhibited the same trend as a standard wind tower. It can be seen that the air supply rates through the wind tower with rotary thermal wheel are approximately one third of the values from the wind tower which correlates to the porosity of the thermal wheel of 70%, added to the reduced area of the casing and this shows that the rotary thermal wheel does not have a significant effect on the air flow through the wind tower and into the room model.

The indoor air temperature measured from the CFD models indicates that at a constant heat output within the building model, there is a noticeable difference between the inlet and exhaust air streams in the wind tower. A recovery of 3°C from the exhaust stream to the inlet stream could generate energy savings up to 20% in heating costs (54). The potential to recover heat through a rotating thermal wheel could lead to further lower energy costs for heating systems due to the increased heat recovery capabilities.

The results of this study show that incorporating a rotary thermal wheel into a standard wind tower does not result in a significant decrease in the air supply rate into a building whereby the ventilation guideline rates are not met. This shows that the concept has significant potential to be developed further, whereby the heat transfer properties of the system can be investigated and tested on a larger scale.

## Acknowledgements

The authors would like to acknowledge and thank the Department of Civil Engineering, University of Leeds for support and use of facilities, the University of Leeds University Research Scholarship for financial support and the University of Leeds SPARK Enterprise Scholarship Programme.

## References

1. DECC. *Climate Change Act*. London, 2008.
2. WBCSD. *Energy Efficiency in Buildings: Facts & Trends*. World Business Council for Sustainable Development 2008.
3. PEREZ-LOMBARDA, L., J. ORTIZ and C. POUT. A review on buildings energy consumption information. *Energy & Buildings*, 2008, **40**(3), pp.394-8.
4. LINDEN, P.F. The fluid mechanics of natural ventilation. *Annual Review of Fluid Mechanics*, 1999, **31**, pp.201-238.
5. HUGHES, B.R. and C.-M. MAK. A study of wind and buoyancy driven flows through commercial wind towers. *Energy and Buildings*, 2011, **43**(7), pp.1784-1791.
6. BOUCHAHM, Y., F. BOURBIA and A. BELHAMRI. Performance analysis and improvement of the use of wind tower in hot dry climate. *Renewable Energy*, 2011, **36**(3), pp.898-906.
7. BAHADORI, M.N. An improved design of wind towers for natural ventilation and passive cooling. *Solar Energy*, 1985, **35**(2), pp.119-29.

8. JONES, B.M. and R. KIRBY. The Performance of Natural Ventilation Windcatchers in Schools - A Comparison between Prediction and Measurement. *International Journal of Ventilation*, 2010, **9**(3), pp.273-286.
9. KOLOKOTRONI, M., B.C. WEBB and S.D. HAYES. Summer cooling with night ventilation for office buildings in moderate climates. *Energy and Buildings*, 1998, **27**(3), pp.231-237.
10. MUMOVIC, D., J. PALMER, M. DAVIES, M. ORME, I. RIDLEY, T. ORESZCZYN, C. JUDD, R. CRITCHLOW, H.A. MEDINA, G. PILMOOR, C. PEARSON and P. WAY. Winter indoor air quality, thermal comfort and acoustic performance of newly built secondary schools in England. *Building and Environment*, 2009, **44**(7), pp.1466-1477.
11. CLEMENTS-CROOME, D.J., H.B. AWBI, Z. BAKO-BIRO, N. KOCHHAR and M. WILLIAMS. Ventilation rates in schools. *Building and Environment*, 2008, **43**(3), pp.362-367.
12. HUGHES, B.R. and S.A.A. ABDUL GHANI. Investigation of a windvent passive ventilation device against current fresh air supply recommendations. *Energy & Buildings*, 2008, **40**(9), pp.1651-9.
13. HUGHES, B.R. and S.A. GHANI. A numerical investigation into the feasibility of a passive-assisted natural ventilation stack device. *International Journal of Sustainable Energy*, 2011, **30**(4), pp.193-211.
14. KIRK, S. and M. KOLOKOTRONI. Windcatchers in Modern UK Buildings: Experimental Study. *International Journal of Ventilation*, 2004, **3**, pp.68-78.
15. LIU, S.C., C.M. MAK and J.L. NIU. Numerical Evaluation of Louver Configuration and Ventilation Strategies for the Windcatcher System. *Building and Environment*, 2011, **46**(8), pp.1600-1616.
16. WALKER, C., T. GANG and L. GLICKSMAN. Reduced-scale building model and numerical investigations to buoyancy-driven natural ventilation. *Energy and Buildings*, 2011, **43**(9), pp.2404-13.
17. MONTAZERI, H., F. MONTAZERI, R. AZIZIAN and S. MOSTAFAVI. Two-sided wind catcher performance evaluation using experimental, numerical and analytical modeling. *Renewable Energy*, 2010, **35**(7), pp.1424-35.
18. MONTAZERI, H. Experimental and numerical study on natural ventilation performance of various multi-opening wind catchers. *Building and Environment*, 2011, **46**(2), pp.370-378.
19. ELMUALIM, A.A. Effect of damper and heat source on wind catcher natural ventilation performance. *Energy and Buildings*, 2006, **38**(8), pp.939-48.
20. SHEA, A.D., A.P. ROBERTSON, G.J. LEVERMORE and N.M. RIDEOUT. Measurements of the performance of a wind-driven ventilation terminal. *Proceedings of the Institution of Civil Engineers: Structures and Buildings*, 2010, **163**(2), pp.129-136.
21. ELMUALIM, A.A. Verification of design calculations of a wind catcher/tower natural ventilation system with performance testing in a real building. *International Journal of Ventilation*, 2006, **4**(4), pp.393-404.
22. BANSAL, N.K., R. MATHUR and M.S. BHANDARI. A Study of Solar Chimney Assisted Wind Tower System for Natural Ventilation in Buildings. *Building and Environment*, 1994, **29**(4), pp.495-500.
23. SHAO, L., S.B. RIFFAT and G. GAN. Heat recovery with low pressure loss for natural ventilation. *Energy and Buildings*, 1998, **28**(2), pp.179-184.
24. WOODS, A.W., S. FITZGERALD and S. LIVERMORE. A comparison of winter pre-heating requirements for natural displacement and natural mixing ventilation. *Energy and Buildings*, 2009, **41**(12), pp.1306-1312.
25. YOUNIS, M. and M. SHOUKRY. REGENERATIVE ROTARY HEAT EXCHANGER FOR HEAT RECOVERY IN RESIDENTIAL VENTILATION. *International Journal of Energy Research*, 1983, **7**(4), pp.315-325.
26. CALAY, R.K. and W.C. WANG. A hybrid energy efficient building ventilation system. *Applied Thermal Engineering*, 2013, **57**(1-2), pp.7-13.

27. CHEN, Q. and J. SREBRIC. A procedure for verification, validation, and reporting of indoor environment CFD analyses. *HVAC and R Research*, 2002, **8**(2), pp.201-216.
28. HUGHES, B.R. and S.A.A.A. GHANI. A numerical investigation into the effect of Windvent louvre external angle on passive stack ventilation performance. *Building and Environment*, 2010, **45**(4), pp.1025-1036.
29. FLUENT. *FLUENT User Guide* [online]. 2006. [Accessed 18/02/2013]. Available from: <http://www1.ansys.com>.
30. CHUNG, J.T. *Computational Fluid Dynamics*. Cambridge: University Press, 2002.
31. CHEN, Q. and L. GLICKSMAN. System Performance Evaluation and Design Guidelines for Displacement Ventilation. *ASHRAE*, 2003.
32. LINDEN, P.F. and P. COOPER. Multiple sources of buoyancy in a naturally ventilated enclosure. *Journal of Fluid Mechanics*, 1996, **311**, pp.177-192.
33. AWBI, H.B. *Ventilation of Buildings*. London: Taylor & Francis, 2003.
34. DEFRAEYE, T., B. BLOCKEN and J. CARMELIET. Convective heat transfer coefficients for exterior building surfaces: Existing correlations and CFD modelling. *Energy Conversion and Management*, 2011, **52**(1), pp.512-522.
35. HOYDYSH, W.G., R.A. GRIFFITHS and Y. OGAWA. A Scale Model Study of the Dispersion of Pollution in Street Canyons. In: *Proceedings of the 67th Annual Meeting of the Air Pollution Control Association*, Denver, USA. 1974.
36. CASTRO, I.P. and A.G. ROBINS. The Flow Around a Surface-Mounted Cube in Uniform and Turbulent Streams. *Journal of Fluid Mechanics*, 1977, **79**(2), pp.307-335.
37. CHERRY, N.J., R. HILLIER and M.E.M.P. LATOUR. Unsteady Measurements in a Separated and Reattaching Flow. *Journal of Fluid Mechanics*, 1984, **144**(Jul), pp.13-46.
38. OHBA, M. Experimental Studies for Effects of Separated Flow on Gaseous Diffusion Around Two Model Buildings. *Journal of Architectural Planning and Environmental Engineering*, 1989, **406**, pp.21-30.
39. DIJILALI, N. and I.S. GARTSHORE. Turbulent Flow Around a Bluff Rectangular Plate Part 1: Experimental Investigation. *Journal of Fluid Engineering*, 1991, **113**, pp.51-59.
40. MOCHIDA, A., S. MURAKAMI and S. KATO. The Similarity Requirements for Wind Tunnel Model Studies of Gas Diffusion. *Journal of Wind Engineering*, 1994, **59**, pp.23-28.
41. UEHERA, K., S. WAKAMATSU and R. OOOKA. Studies on the Critical Reynolds Number Indices for Wind-Tunnel Experiments on Flow within Urban Areas. *Boundary Layer Meteorology*, 2003, **107**(2), pp.353-370.
42. CALAUTIT, J.K., H.N. CHAUDHRY, B.R. HUGHES and L.F. SIM. A validated design methodology for a closed-loop subsonic wind tunnel. *Journal of Wind Engineering and Industrial Aerodynamics*, 2014, **125**, pp.180-194.
43. AL-GHAMDI, A.S. *Analysis of Air-To-Air Rotary Energy Wheels*. Ohio University, 2006.
44. PARKINSON, G.V. and N.J. COOK. Blockage Tolerance of a Boundary-Layer Wind-Tunnel. *Journal of Wind Engineering and Industrial Aerodynamics*, 1992, **42**(1-3), pp.873-884.
45. GLANVILLE, M.J. and K.C.S. KWOK. Further investigation of the blockage-tolerant wind tunnel technique. *Journal of Wind Engineering and Industrial Aerodynamics*, 1997, **71**, pp.987-995.
46. CHENG, Y., F.S. LIEN, E. YEE and R. SINCLAIR. A comparison of large Eddy simulations with a standard k- $\epsilon$  Reynolds-averaged Navier-Stokes model for the prediction of a fully developed turbulent flow over a matrix of cubes. *Journal of Wind Engineering and Industrial Aerodynamics*, 2003, **91**, pp.1301-1328.
47. JIANG, Y. and Q. CHEN. Study of natural ventilation in buildings by large eddy simulation. *Journal of Wind Engineering and Industrial Aerodynamics*, 2001, **89**(13), pp.1155-1178.
48. DFES. *Building Bulletin 101 - Ventilation for School Buildings*. 2006.
49. CIBSE. *Guide B: Heating, Ventilating, Air Conditioning and Refrigeration* London: Chartered Institution of Building Service Engineers, 2005.



50. DATABASE/BERR, U.W.S. *Annual Mean Wind Speed at 25m Above Ground Level*. 2008.
51. MARDIANA, A., S.B. RIFFAT and M. WORALL. Integrated heat recovery system with wind-catcher for building applications: towards energy-efficient technologies. *Materials and processes for energy: communicating current research and technological developments*, 2013.
52. OFFICE, M. *Averages Table - UK - Climate Period: 1981-2010* [online]. 2013. [Accessed 20/11/2013]. Available from: <http://www.metoffice.gov.uk/>.
53. SREBRIC, J. and Q. CHEN. An example of verification, validation, and reporting of indoor environment CFD analyses. In: *ASHRAE Transactions 2002, June 22, 2002 - June 26, 2002*, Honolulu, HI, United states. Amer. Soc. Heating, Ref. Air-Conditioning Eng. Inc., 2002, pp.185-194.
54. WBCSD. *Energy efficiency in buildings: transforming the market*. World Business Council for Sustainable Development 2009.